A Novel Interferometric Millimeter Wave Doppler Radar Architecture

Shaolin Liao*, N. Gopalsami, S. Bakhtiari, T. Elmer, and A. C. Raptis

Nuclear Engineering Division

Argonne National Laboratory

9700 S. Cass Avenue, Lemont, IL, 60439

*sliao@anl.gov

***Abstract*—A universal, mixerless millimeter wave (mmW) Doppler radar architecture consisting of simply a Continuous Wave (CW) source and an intensity detector based on optical interferometry technique has been assembled. The phase information is obtained by using an oscillating mirror in the reference arm, similar to that used by the FTIR (Fourier Transform Infrared spectroscopy) technique. The reference mirror oscillates at a frequency that is higher than twice the Doppler frequency of the object. Rigorous mathematical formulas have been derived to solve for both the amplitude and the phase of the Doppler signal, by using the Low-Frequency-Band (LFB) and High-Frequency-Band (HFB) signals. The Doppler frequency signature of a moving object can be obtained from the Fourier transform of the phase. A prototype at 94 GHz was built and tested using a ball pendulum target moving over a full-swing distance much smaller than a wavelength. Both the measured amplitude and phase have been shown to agree well with the experimental parameters. The interferometric Doppler radar architecture is universal and can be extended to THz without significant change of components.**

Keywords—millimeter wave, THz, Doppler, Radar, CW, Michelson interferometry

I. INTRODUCTION

Doppler sensors have been extensively investigated in the microwave [1-4] and optics [5-7] range. At microwave frequencies, Doppler sensors are usually realized through the use of quadrature mixers. Microwave devices have inherently lower sensitivity (micrometer displacements) than their optical counterparts. High-frequency optical sensors suffer from alignment and diffraction loss due to surface roughness and thus not best suited for detection of complex objects. Furthermore, optical wavelengths cannot penetrate through opaque cover materials such as fabrics, plastics and insulation layers on many common targets of interest. To make use of the advantages provided by both low-frequency microwaves and high-frequency optics, quadrature mixer based mmW Doppler radar has been recently studied for vibrometry is remote monitoring of vital signs [8-9]. Here we investigate a universal, mixerless millimeter wave Doppler radar, based on optical interferometry technique by using a CW source and an intensity detector. The Doppler radar employs a fast oscillating mirror in the reference arm. The detected intensity is the coherent addition of the reference beam and the reflected signal, which features a fast reference modulation on a slow modulation induced by the object. We have derived a rigorous mathematical formulation to solve for both the amplitude and the phase simultaneously. After the phase is obtained, Fourier transform can be used to study the Doppler frequency signature of a moving object. We have built a 94 GHz prototype and an experimental test apparatus using a ball pendulum target with full-swing distance much smaller than a wavelength to study the performance of the proposed interferometric Doppler radar.

II. PRINCIPLE OF THE INTERFEROMETRIC DOPPLER RADAR

A. Architecture of the Interferometric Doppler Radar

Fig. 1 shows the architecture of the Doppler radar, which is based on the Michelson interferometry optical technique using a CW source and an intensity detector. The source wave is first collimated into a parallel beam, which is then split into two beams, with one propagating towards the moving object and the other serving as the reference beam modulated by an oscillating mirror. The reflected Doppler signal by the moving object (blue beam in Fig. 1) is then combined with the reference beam (green beam in Fig. 1) and fed into an intensity detector. A LabVIEW® program is used to collect and process the data.

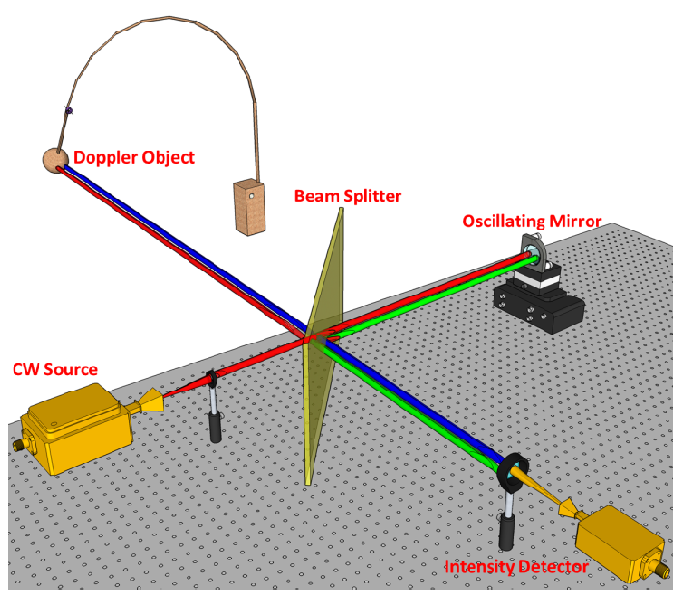

Figure 1. Schematics of the proposed interferometric Doppler radar architecture with just a CW source and an intensity detector.

B. Fundamental Principle

Mathematically, the intensity detector measures the combined reflected signal from the object $E_{obj}(t)$ and the reference beam $E_{ref}(t)$,

$$E(t) = E_{obj}(t) + E_{ref}(t) = a_{obj}(t)e^{j\phi_{obj}(t)} + a_{ref}e^{j\phi_{ref}(t)} \quad (1)$$

where $a_{obj}(t)$ and a_{ref} are the amplitudes of the reflected signal and the reference beam respectively. The corresponding phases are $\phi_{obj}(t)$ and $\phi_{ref}(t)$, respectively. The detected intensity is thus given by

$$I(t) = |E(t)|^2 = a_{obj}^2(t) + a_{ref}^2 + 2a_{ref}a_{obj}(t)\cos[\phi_{ref}(t) - \phi_{obj}(t)] \quad (2)$$

C. LFB and HFB Signals

The intensity signal given in Eq. (2) can be separated into LFB (Low-Frequency-Band) and HFB (High-Frequency-Band) signals. To illustrate this, let us decompose the reference phase $\phi_{ref}(t)$ into Fourier series,

$$\phi_{ref}(t) = \phi_0 + \sum_{m=1}^{\infty} c_m \cos(m\omega_{ref}t) \quad (3)$$

Substituting Eq. (3) into the last term in Eq. (2), one gets

$$\begin{aligned}
2a_{ref}a_{obj}(t)\cos[\phi_{ref}(t) - \phi_{obj}(t)] &= a_{ref}a_{obj}(t)\left\{e^{j(\phi_{ref}(t)-\phi_{obj}(t))} + e^{-j(\phi_{ref}(t)-\phi_{obj}(t))}\right\} \\
&= a_{ref}a_{obj}(t)\left\{\begin{array}{l} e^{-j\tilde{\phi}_{obj}(t)}e^{j\sum_{m=1}^{\infty} c_m\cos(m\omega_{ref}t)} \\ + e^{j\tilde{\phi}_{obj}(t)}e^{-j\sum_{m=1}^{\infty} c_m\cos(m\omega_{ref}t)} \end{array}\right\} \\
&= a_{ref}a_{obj}(t)\left\{\begin{array}{l} e^{-j\tilde{\phi}_{obj}(t)}\prod_{m=1}^{\infty}\left[\begin{array}{l} J_0(c_m) \\ + 2\sum_{n=1}^{\infty}\left[j^n J_n(c_m)\cos(nm\omega_{ref}t)\right] \end{array}\right] \\ + e^{j\tilde{\phi}_{obj}(t)}\prod_{m=1}^{\infty}\left[\begin{array}{l} J_0(c_m) \\ + 2\sum_{n=1}^{\infty}\left[(-j)^n J_n(c_m)\cos(nm\omega_{ref}t)\right] \end{array}\right] \end{array}\right\}
\end{aligned} \quad (4)$$

where Jacobi-Anger expansion has been used to derive Eq. (4). J_0 is Bessel function of the first kind of order 0 and $\tilde{\phi}_{obj}(t) = \phi_{obj}(t) - \phi_0$.

1) LFB signal

The LFB signal from Eq. (4) is given by

$$2a_{ref}a_{obj}(t)\cos[\phi_{ref}(t) - \tilde{\phi}_{obj}(t)]\Big|_{LFB} \approx 2a_{ref}a_{obj}(t)\cos(\tilde{\phi}_{obj}(t))\prod_{m=1}^{\infty} J_0(c_m) \quad (5)$$

Hence, the intensity given in Eq. (2) has the approximate LFB signal of

$$I(t)\big|_{LFB} \approx a_{obj}^2(t) + a_{ref}^2 + 2a_{ref}\prod_{m=1}^{\infty} J_0(c_m)a_{obj}(t)\cos(\tilde{\phi}_{obj}(t)) \quad (6)$$

2) HFB signal

The HFB signal of the following term in Eq. (2) is given by

$$2a_{ref}a_{obj}(t)\cos[\phi_{ref}(t) - \tilde{\phi}_{obj}(t)]\Big|_{HFB} \approx 4a_{ref}J_1(c_1)\prod_{m=2}^{\infty} J_0(c_m)a_{obj}(t)\sin(\tilde{\phi}_{obj}(t))\cos(\omega_{ref}t) \quad (7)$$

from which we obtain the approximate amplitude of the HFB,

$$I(t)\big|_{HFB} \approx 4a_{ref}J_1(c_1)\prod_{m=2}^{\infty} J_0(c_m)a_{obj}(t)\sin(\tilde{\phi}_{obj}(t)) \quad (8)$$

D. Amplitude and Phase

The amplitude and phase of the object can be solved from the LFB signal in Eq. (6) and HFB signal in Eq. (8),

$$x_c(t)^2 + Bx_c(t) + C = 0 \quad (9)$$

where we have the following definitions:

$$\begin{aligned}
x_c(t) &\equiv a_{obj}(t)\cos(\tilde{\phi}_{obj}(t)) \\
B &= 2a_{ref}\prod_{m=1}^{\infty} J_0(c_m) \\
C &= a_{ref}^2 + x_s(t)^2 - I(t)\big|_{LFB} \\
x_s(t) &\equiv a_{obj}(t)\sin(\tilde{\phi}_{obj}(t)) \\
&= I(t)\big|_{HFB} \Big/ 4a_{ref}J_1(c_1)\prod_{m=2}^{\infty} J_0(c_m)
\end{aligned} \quad (10)$$

The variable $x_c(t)$ can be solved from Eq. (11),

$$x_c(t) = \frac{-B \pm \sqrt{B^2 - 4C}}{2} \quad (11)$$

Combining Eq. (9) and Eq. (11), we obtain the amplitude and phase

$$a_{obj}(t) = \sqrt{x_c(t)^2 + x_s(t)^2}\,;\ \tilde{\phi}_{obj}(t) = \arctan\left[x_s(t) \big/ x_c(t) \right] \quad (12)$$

E. Doppler Signature

After we obtain the complex-valued reflected Doppler signal complex field (amplitude and phase), we can analyze the Doppler frequency signature of the moving object. The Doppler frequency $f_{Doppler}(t)$ from the carrier frequency f is given by

$$f_{Doppler}(t) = 2\frac{v(t)}{c}f \quad (13)$$

where $v(t)$ is the object velocity and c is the speed of light. The Doppler frequency is closely related to the phase $\phi_{obj}(t)$ of the reflected signal for the object displacement $x(t)$,

$$f_{Doppler}(t) = \frac{d\phi_{obj}(t)}{dt} = \frac{4\pi}{\lambda}\frac{dx(t)}{dt} \quad (14)$$

where λ is the carrier wavelength. Eq. (14) has taken into account the round trip of the carrier wave.

III. Experimental Result

A. Experimental Description

To test the performance of the proposed interferometric Doppler radar, we built a 94 GHz prototype using a Gunn oscillator as source and a Schottky Barrier (SB) diode as intensity detector. The reference mirror is oscillating at a frequency of 200 Hz with displacement amplitude of $A_{mirror} \approx 0.03$ mm, which is much smaller than the wavelength of $\lambda \approx 3.2$ mm. This corresponds to the following parameters in Eq. (4): $c_1 = 4\pi A_{mirror} \big/ \lambda \approx 0.1181$, $J_1(c_1) \approx 0.0588$, $J_1(c_m) \approx 0, m = 2,3,4...; c_m \approx 0, J_0(c_m) \approx 1, m = 1,2,3...$. During the experiment, a swinging ball pendulum with length $L \approx 15$ cm was used as the moving object, giving a swing frequency of $f_{pendulum} \approx \frac{1}{2\pi}\sqrt{\frac{g}{L}} = \frac{1}{2\pi}\sqrt{\frac{9.8}{L}} \approx 1.286$ Hz. The full swing distance of the pendulum was set to $D_{pendulum} = 0.25$ mm, much smaller than the carrier wavelength of $\lambda \approx 3.2$ mm.

B. Experimental Result and Analysis

A sample segment of the measured intensity $I(t)$ is shown in Fig. 2. The signal before approximately 45s was collected with the reference mirror oscillating at 200 Hz. The reference mirror is kept stationary after approximately 45s. Fig. 3 shows the close up of a small segment of the measured intensity $I(t)$ shown in Fig. 2. The 200 Hz modulation is evident before approximately 45s with no modulation when the reference mirror ceased to oscillate after approximately 45s.

The LFB signal given in Eq. (6) and HFB signal given in Eq. (8) are shown in Fig. 4a) and Fig. 4b) respectively.

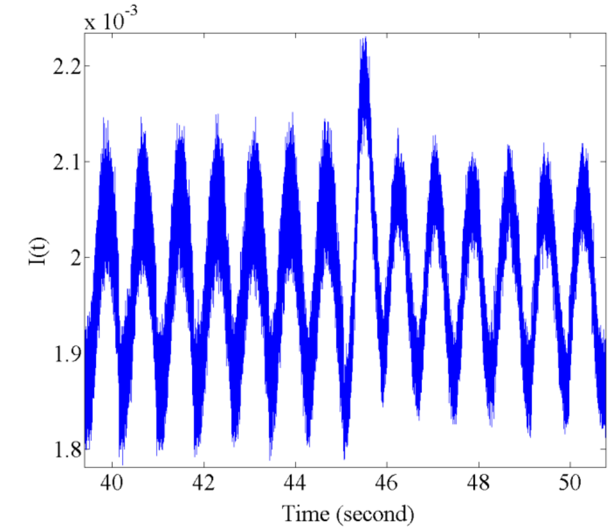

Figure 2. Measured intensity $I(t)$ for a ball pendulum of small amplitude.

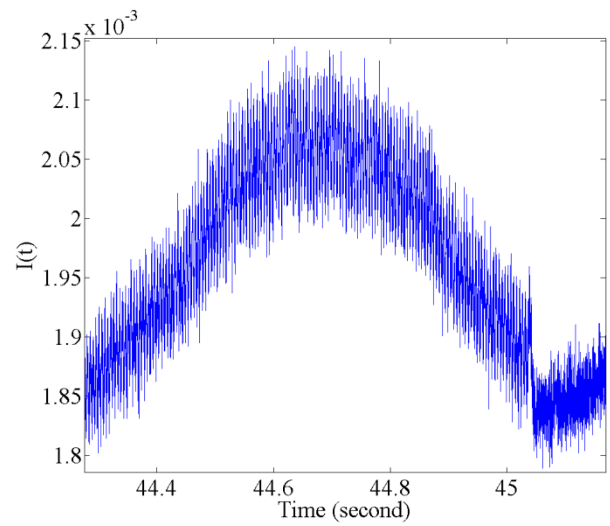

Figure 3. A zoom view of a small segment of $I(t)$ in Fig. 2 to show the 200 Hz modulation of one single cycle for approximately $t < 45$ seconds.

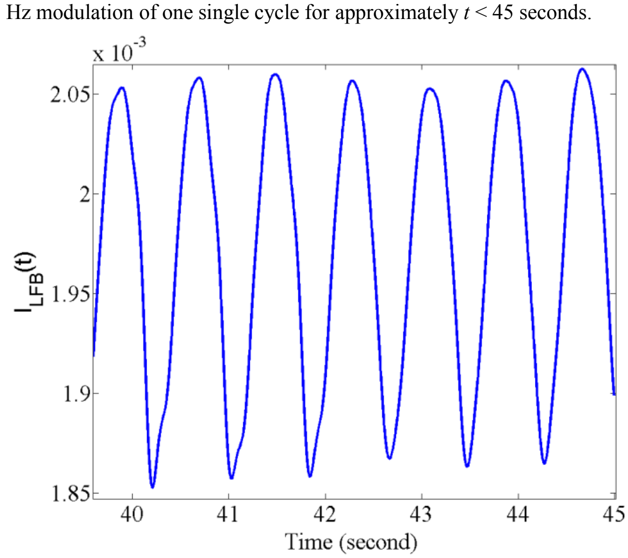

(a)

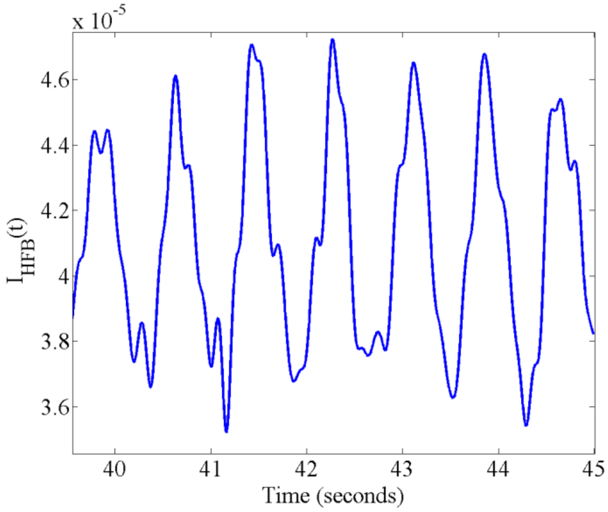

(b)

Figure 4. a) LFB signal from Eq. (6), and b) HFB signal from Eq. (8).

With LFB and HFB signals now available, the amplitude and phase can be obtained by solving Eq. (9) to Eq. (12) with the results shown in Fig. 5. The displacement amplitude of the object $a_{obj}(t)$ is shown in Fig. 5a), which has a mean value of $\overline{a}_{obj}(t) = 0.0028$. Fig. 5b) shows the displacement phase of the object $\phi_{obj}(t)$. The full-swing phase, i.e., difference between phase maximum $\phi_{obj}(t)\big|_{\max}$ and phase minimum $\phi_{obj}(t)\big|_{\min}$, is $\approx 58°$, which corresponds to a full-swing distance of $D_{measured} \approx 0.2571$ mm, agreeing well with the experimentally set swing value of $D_{pendulum} = 0.25$ mm. The Doppler frequency signature can be obtained by taking the Fourier transform of $\phi_{obj}(t)$ given in Fig. 5b). The result of the transformation is shown in Fig. 6. The measured pendulum frequency is $f_{measured} \approx 1.275$ Hz, agreeing well with the theoretically calculated value of $f_{pendulum} \approx 1.286$ Hz. Finally, the sensitivity of the 94-GHz prototype was determined to be ~5 degrees, which corresponding to ~45 μm displacement accuracy.

IV. Discussion

The interferometric Doppler radar architecture described above is universal in that it can be implemented over the entire mmW to THz range. Although a mmW (94-GHz) prototype was built to perform proof of concept study of this novel interferometric Doppler radar architecture, a THz prototype can readily be built by replacing only the CW source and the intensity detector. For example, as THz source either a Backward Wave Oscillator (BWO) or a THz Quantum Cascade Laser (QCL) could replace the mmW Gunn Oscillator and as intensity detector either a pyroelectric detector or a Hot Electron Bolometer (HEB) can be used. The mmW/THz

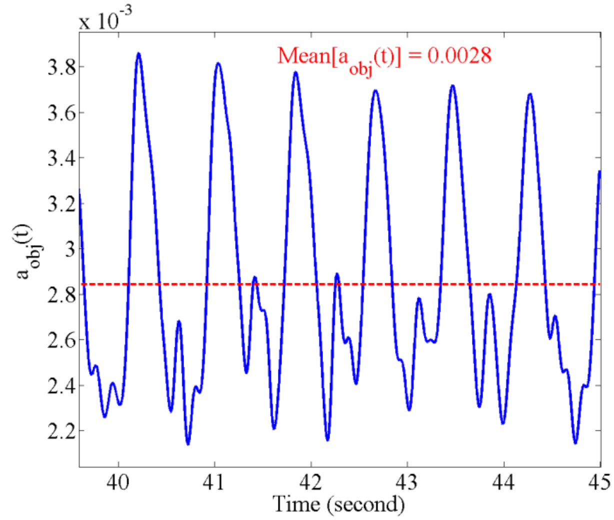

(a)

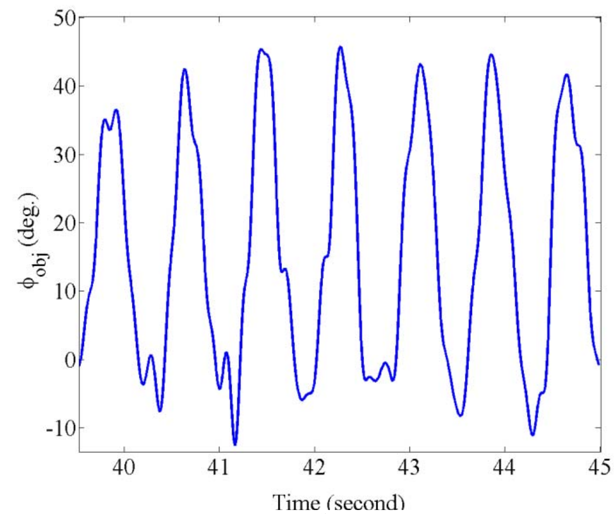

(b)

Figure 5. a) amplitude $a_{obj}(t)$, and b) phase $\phi_{obj}(t)$.

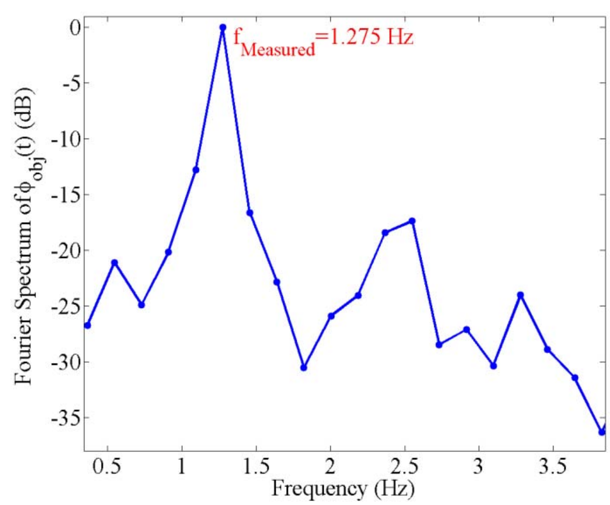

Figure 6. Doppler signature: Fourier transform of $\phi_{obj}(t)$ given in Fig. 5.

interferometric Doppler radar has many applications, including vibration/displacement measurement (down to few μm), coating/thin film thickness measurement, dielectric constant characterization, phase-sensitive chemicals spectroscopy and phase-contrast Non-Destructive Evaluation (NDE) of dielectric materials.

V. Conclusion

We studied a universal, mixerless interferometric Doppler radar architecture employing a CW source and an intensity detector. A motorized oscillating reference mirror is used to modulate the intensity at a frequency higher than twice the object's Doppler frequency. A rigorous mathematical formulation was derived to extract both the amplitude and the phase of the Doppler signal by decomposing the measured intensity into LFB and HFB signals. A 94-GHz prototype was built and tested using a ball pendulum target with a full-swing distance much smaller than the carrier wavelength. The measurement results were shown to agree well with the experimentally adjusted parameters such as pendulum frequency and full-swing distance. It is expected that this novel Doppler architecture can be readily extended to the THz range for a wide range of remote sensing applications requiring phase-sensitive measurement.

VI. Acknowledgement

This work is sponsored by National Nuclear Security Administration of Department of Energy under contract No. DE-AC02-06CH11357.

References

[1] Lubecke V., Lin Jenshan, and Boric-Lubecke, O., "A microwave radio for Doppler radar sensing of vital signs," *Microwave Symposium Digest, 2001 IEEE MTT-S International*, Vol. 1, pp 175-178 (2001).

[2] Boric-Lubecke O., Ong P. W., and Lubecke V. M., "10 GHz Doppler sensing of respiration and heart movement," in *Proc. IEEE 28th Annu. Northeast Bioeng. Conf.*, Philadelphia, PA, pp. 55–56 (2002).

[3] Obeid D., Sadek S., Zaharia G., and El-Zein G., "Non-contact heartbeat detection at 2.4, 5.8 and 60 GHz: A comparative study," *Microw. Opt. Technol. Lett.*, Vol. 51, No. 3, pp. 666–669 (2009).

[4] Obeid D., Zaharia G., Sadek S., and Zein G. E., "Microwave Doppler radar for heartbeat detection vs. electrocardiogram," *Microwave and Optical Technology Letters*, Vol. 54, Iss. 11, pp 2610-2617 (2012).

[5] Roos P. A., Stephens M., and Wieman C. E., "Laser vibrometer based on optical-feedback-induced frequency modulation of a single-mode laser diode," *Applied Optics*, Vol. 35, No. 34, pp. 6754-6761 (1996).

[6] Nassif H. H., Gindy M., and Davis J., "Comparison of laser Doppler vibrometer with contact sensors for monitoring bridge deflection and vibration," *NDT & E International*, Vol. 38, Iss. 3, pp. 213-218 (2005).

[7] Wang C.-C., Trivedi S., Jin F., Swaminathan V., Rodriguez P., and Prasad N. S., "High sensitivity pulsed laser vibrometer and its applicatoin as a laser microphone," *Applied Physics Letters* 94, 051112 (2009).

[8] Bakhtiari S., Liao, S., Elmer, T. W., Gopalsami, N., and Raptis, A. C., "A Real-Time Heart Rate Analysis for a Remote Millimeter Wave I-Q Sensor," *IEEE Trans. On Biomedical Engineering*, Vol. 58, pp. 1839-1845 (2011).

[9] Mikhelson I. V., Bakhtiari, S., Elmer, T. W., Sahakian, A. V., "Remote Sensing of Heart Rate and Patterns of Respiration on a Stationary Subject Using 94-GHz Millimeter-Wave Interferometry," *IEEE Transactions on Biomedical Engineering*, Vol. 58, No. 6, pp. 1671-1677 (2011).